COGNITIVE NEUROSCIENCE

Motifs of human high-frequency oscillations structure processing and memory of continuous audiovisual narratives

Akash Mishra[1,2]*, Gelana Tostaeva[1], Maximilian Nentwich[1], Elizabeth Espinal[1,3], Noah Markowitz[1], Jalen Winfield[1], Elisabeth Freund[1], Sabina Gherman[1], Marcin Leszczynski[4,5], Charles E. Schroeder[4,6], Ashesh D. Mehta[1,2], Stephan Bickel[1,2,6]*

The discrete events of our narrative experience are organized by the neural substrate that underlies episodic memory. This narrative process is segmented into distinct units by event boundaries, which facilitate a replay process that acts to consolidate each event into a narrative memory. High-frequency oscillations (HFOs) may synchronize neural activity during these processes. We use intracranial recordings from participants viewing and freely recalling a continuous, audiovisual stimulus. We find that hippocampal HFOs increase following event boundaries and hippocampal-cortical coincident HFOs (co-HFOs) occur in cortical regions that underlie event segmentation (inferior parietal, precuneus, lateral occipital, and inferior frontal cortices). Event-specific co-HFO patterns that occur during event viewing reoccur following event boundaries for the subsequent three events and during recall. This is consistent with models that support replay as a mechanism for memory consolidation. Therefore, HFOs may coordinate activity across brain regions that facilitate event segmentation, encode memory of discrete events, and bind representations to assemble memory of a coherent, continuous experience.

INTRODUCTION

Despite our daily immersion in continuous, multimodal experiences, we tend to recall memories as episodic events (*1*). These "real-life" narratives facilitate connections with other experienced events to generate memory scaffolds (*2*). We have an insufficient understanding of how the human brain segments a continuous narrative, coordinates the activation of widespread memory-containing cortical regions, and integrates events experienced over time (*3*–*5*). It is likely that these processes rely on a synchronizing mechanism that organizes several brain regions, including the hippocampus, sensory cortices, and widespread cortical regions that process and store multimodal memories.

A continuous narrative may be divided into discrete events by event boundaries or time points that are associated with contextual shifts (*6*, *7*). This process is supported by an event segmentation hierarchy that spans lower-level sensory regions and higher-order, multimodal processing regions (*8*). Critically, different levels of this assembly are receptive to varying degrees of event granularity: sensory regions are more responsive to finer boundaries, whereas multimodal integration regions are more responsive to abstract, coarse boundaries (*8*–*10*). The critical process of recapitulating event representations from previously experienced events, or "replay," occurs following event boundaries; hence, this may represent an optimal window for the consolidation of memory for continuous stimuli (*7*, *11*). Several studies have suggested that the hippocampus may play a role in coordinating event segmentation and memory processes during this window (*7*, *8*, *11*–*15*). However, the mechanisms underlying this are not well understood.

Physiological 80- to 140-Hz high-frequency oscillations (HFOs) have been implicated in the recruitment of memory-containing cortical regions (*16*–*21*), especially during the replay of previously-experienced events (*22*, *23*). HFOs that occur at the same time in different brain regions [coincident HFOs ("co-HFOs")] may synchronize brain regions in the memory network (*18*, *21*, *24*–*27*) by eliciting specific patterns of neuronal firing (*19*). Because the memory of continuous narratives likely requires widespread, brain-wide coordination, HFOs may serve as an optimal potential coordinating mechanism underlying this process. We hypothesize that co-HFOs bind hippocampal-cortical activity in cortical regions previously found in functional magnetic resonance imaging (fMRI) studies to be involved in event segmentation (for example, angular gyrus, precuneus, and lateral occipital cortex) (*8*, *28*). Furthermore, on the basis of scalp electroencephalography (EEG) (*29*, *30*) and fMRI (*28*) studies showing similarity in brain activity between event viewing and following event boundaries, we expect HFOs to exhibit specific spatial and temporal patterns of coincidence across the hippocampus and cortex ("co-HFO motifs") that demonstrate similarity in the processes of event encoding (viewing), replay (following event boundaries), and memory retrieval (recall). As ensembles of micro- and mesoscale HFOs may serve as engrams for memory processes (*31*), these co-HFO motifs would be unique for each event. In addition, because memory processes scaffold upon several previously viewed events, they would contain representations for both the most recently viewed event and several events prior.

In this study, we recorded intracranial electrophysiological data from patients who watched a 10-min clip of the cartoon Despicable Me and then performed a free recall of their event memory. We leverage the spatial and temporal resolution of intracranial EEG (iEEG)

[1]The Feinstein Institutes for Medical Research, Northwell Health, Manhasset, NY, USA. [2]Departments of Neurosurgery and Neurology, Zucker School of Medicine at Hofstra/Northwell, Hempstead, NY, USA. [3]Department of Psychological and Brain Sciences, Drexel University, Philadelphia, PA, USA. [4]Department of Psychiatry, Columbia University College of Physicians and Surgeons, New York, NY, USA. [5]Center for Cognitive Science, Faculty of Philosophy, Jagiellonian University, Kraków, Poland. [6]Center for Biomedical Imaging and Neuromodulation, Nathan Kline Institute, Orangeburg, NY, USA.
*Corresponding author. Email: amishra4@northwell.edu (A.M.); sbickel@northwell.edu (S.B.)

to show that hippocampal HFOs (hHFOs) increase in rate following event boundaries, and this activation is most prominent in right-anterior hippocampal electrodes. Hippocampal-cortical co-HFOs increase in a wide cortical network, with the most prominent increases present in regions that show activation at event boundaries in prior fMRI studies (*8*, *28*). We identify event-specific spatial and temporal patterns of HFOs (co-HFO motifs) that recur following event boundaries and during event free recall. The magnitude of pattern reactivation for an event diminishes as additional events are viewed. Together, HFOs represent a potential mechanism of synchronizing activity across the expansive hippocampal-cortical memory network and may underlie how humans process continuous, real-life stimuli as a sequence of events. This process may be associated with event-specific arrangements of co-HFOs that are present during event viewing and reactivate at times of memory function.

RESULTS

The aim of this study was to investigate HFOs as a mechanism underlying multiregional synchrony at event boundaries. To answer this, we recorded iEEG from 32 testing sessions (30 participants), while they watched a 10-min clip of the film Despicable Me (Fig. 1A). Nine event boundaries with high interparticipant consistency (*32*) were used. Twelve participants were additionally asked to freely recall details from the clip. Participants recalled an average of 55.8 ± 17.8% of events (Fig. 1B).

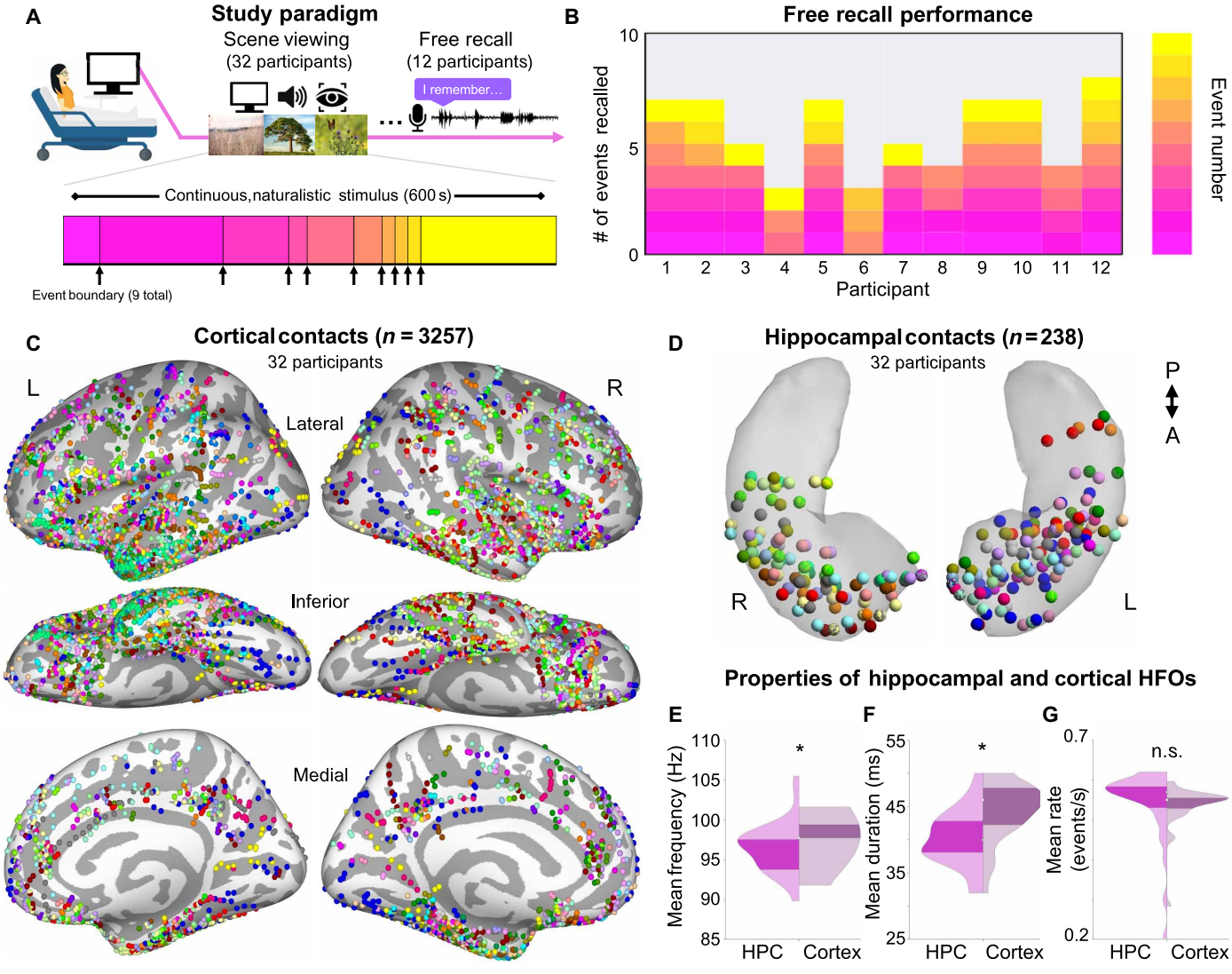

Fig. 1. Experimental design, recording contacts, and HFO detection. (**A**) Experimental design. Participants ($n = 32$) viewed a 10-min continuous clip of the film Despicable Me. The clip was segmented into 10 events by 9 event boundaries. Following this, a subset of participants ($n = 12$) performed a free recall describing what they remembered from the clip. The images shown are different from those used in the experiment and are sourced from Unsplash. (**B**) Chart detailing content of recall for all 12 participants who performed free recall. (**C**) Cortical contact locations across participants on a standard inflated brain surface. Each color represents one unique participant. (**D**) Locations of hippocampal contacts across participants on a hippocampal surface of a standard brain. Each color represents contacts from individual participants. (**E** to **G**) Distribution of hippocampal and cortical HFO (E) peak frequency, (F) duration, and (G) rate across $n = 3257$ cortical contacts and $n = 238$ hippocampal contacts ($n = 32$ participants). *$P < 0.05$, Student's t test. n.s., not significant; L, left; R, right; A, anterior; P, posterior.

Properties of hippocampal and cortical HFOs

We examined HFOs during scene viewing (3257 cortical and 238 hippocampal contacts across 32 sessions) (Fig. 1, C and D) and free recall (1075 cortical and 90 hippocampal contacts across 12 sessions) (fig. S1). Across participants, detected HFO events during viewing in hippocampal and cortical contacts significantly differed in peak frequency (median of 97.6 Hz in the hippocampus and 97.7 Hz in the cortex; $n = 32$ participants, signed-rank $z = 3.021$, $P = 0.003$; Fig. 1E) and duration (median of 40 ms in the hippocampus and 46 ms in the cortex; $n = 32$ participants, signed-rank $z = 3.518$, $P < 0.001$; Fig. 1F) but did not significantly differ in rate (median of 0.57 events/s in the hippocampus and 0.55 events/s in the cortex; signed-rank $z = 1.664$, $P = 0.096$; Fig. 1G). The grand average field potential, spectral power, inter-HFO interval, and rate across time for hHFOs are illustrated in fig. S2. Cortical HFO characteristics are roughly stable across cortical regions (fig. S3).

Hippocampal HFOs during scene viewing and recall

Event boundaries may serve as a period of increased hippocampal-cortical coordination for the consolidation of previously viewed events. Hence, we examined the relationship between hHFOs and event boundaries. We constructed an event boundary-locked perievent time histogram (PETH) across all participant and hippocampal contacts. This was compared to a PETH derived from visually and auditory-matched control scenes (fig. S4). Hippocampal HFO rate increased transiently but significantly 1 to 2 s following event boundaries ($P = 0.026$, cluster-based permutation test; Fig. 2A). This increase was also significant on the group level [median post-boundary HFO rate across $n = 32$ participants of 0.618 events/s compared to preboundary baseline rate of 0.517 events/s: signed-rank $z = 2.387$, $P = 0.017$, Hedge's $g = 0.372$ (fig. S5A); postboundary duration to median HFO rate during matched control scenes of 0.527 events/s: signed-rank $z = 1.803$, $P = 0.071$, Hedge's $g = 0.256$ (fig. S5B)]. For participants who performed free recall, scenes that were subsequently recalled demonstrated a trend toward increased hHFO rate in this postevent boundary window compared to scenes that were not subsequently recalled [$n = 12$ participants, $P < 0.07$ (fig. S6); group-level median normalized correlation coefficient after boundary of 0.141 compared to −0.055 in matched preboundary period, Hedge's $g = 2.47$]. This supports the hypothesis that hHFOs play a role in replay processes in the period following event boundaries (*33*). Next, we aimed to assess which hippocampal contacts contribute to this phenomenon. We calculated the magnitude of HFO rate increase following event boundaries for each contact (2-s window following event boundaries compared to 2-s window prior) (Fig. 2B). Then, we implemented a general linear regression model with the following factors: hippocampal subfield (CA1 or non-CA1), longitudinal position along the hippocampus (median split by participant; anterior or posterior), and brain hemisphere (left or right). Interaction effects between factors were included. We found a significant link between postevent boundary HFO rate increases and (i) hippocampal contacts in the CA1 subfield ($t = 1.900$, $P = 0.029$) and (ii) the interaction between right hemisphere and anterior hippocampus ($t = 1.912$, $P = 0.031$) (Fig. 2C). We further quantified the effect of longitudinal axis and hemisphere and found a significant postboundary hHFO rate increase in 65 right-anterior hippocampal contacts [one-sample $t(64) = 2.828$, Bonferroni-corrected $P = 0.006$, Hedge's $g = 0.351$] but not in 53 left-anterior hippocampal

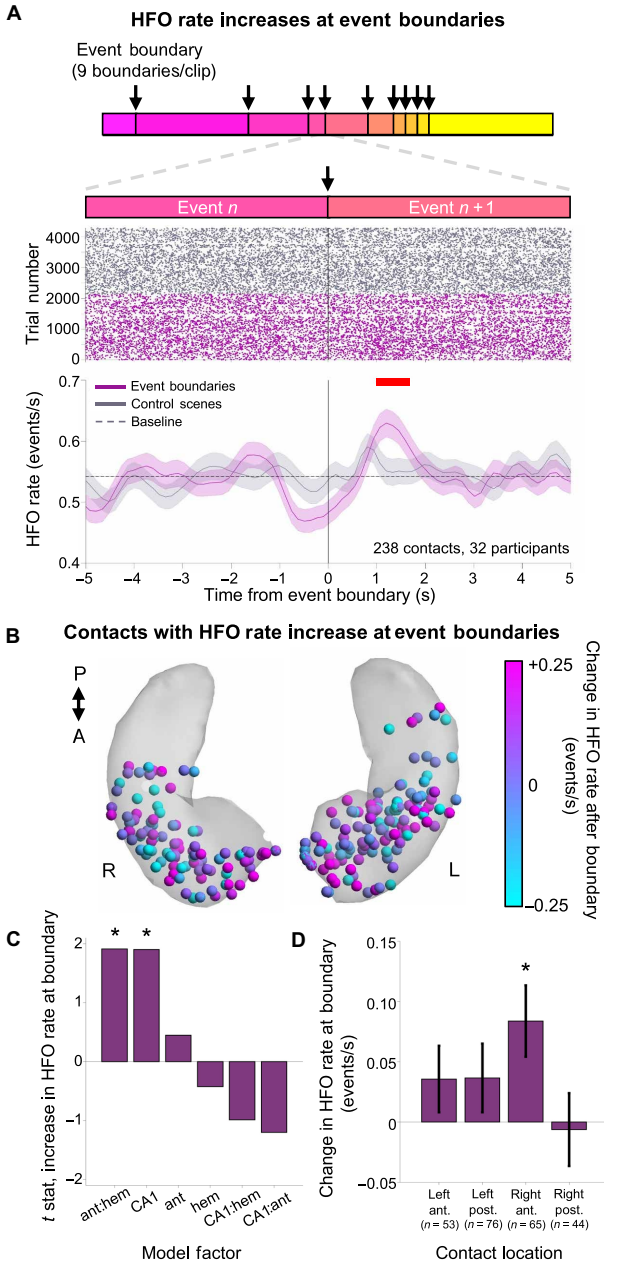

Fig. 2. Hippocampal HFOs increase after event boundaries. (**A**) Hippocampal HFO rate raster plot and PETH time-locked to event boundaries (pink) and auditory- and visually matched control scenes (gray) ($n = 238$ contacts, $n = 32$ participants, and $n = 9$ event boundaries). Red line indicates significance at $P < 0.05$ (permutation test compared to shuffled hHFO timings in the same epoch). Shaded areas represent 1 bootstrap SEM computed over hHFO events. Dashed line represents the mean hHFO rate over this epoch. (**B**) Magnitude of change in hHFO rate following event boundaries (compared to before the boundary) for each hippocampal contact on a normalized hippocampal surface. Warmer colors indicate greater increase in hHFO rate. (**C**) *t* values obtained from a generalized linear model assessing the characteristics of hippocampal contacts that are associated with increases in hHFO rate following event boundaries. Factors tested were longitudinal axis (ant), hemisphere (hem), and CA1 subfield (CA1). *$P < 0.05$ for the model term or interaction effect. (**D**) Mean change in hHFO rate following event boundaries (compared to before boundaries) for hippocampal contacts, divided by hemisphere and longitudinal axis of the hippocampus. Error bars represent 1 SEM. *$P < 0.05$, Bonferroni-corrected, one-sample *t* test.

contacts [$t(52) = 1.291$, Bonferroni-corrected $P = 0.202$, Hedge's $g = 0.177$], 76 left-posterior hippocampal contacts [$t(75) = 1.283$, Bonferroni-corrected $P = 0.203$, Hedge's $g = 0.147$], or 44 right-posterior hippocampal contacts [$t(43) = -0.209$, Bonferroni-corrected $P = 0.836$, Hedge's $g = 0.032$]. To test whether this relationship holds true on the participant level, we selected $n = 21$ participants who had at least one right-anterior hippocampal contact and at least one other hippocampal contact. Right-anterior contacts were found to exhibit a mean increase in HFO rate after event boundaries of 0.069 events/s, compared to 0.022 events/s for all other hippocampal contacts. This increase trended toward significance ($P = 0.104$, permutation test shuffling hippocampal electrode labels within participants; Hedge's $g = 0.341$).

Last, as hHFOs may represent an electrophysiological marker for the recruitment of memory-containing regions during memory retrieval before onset of free recall, we created a PETH locked to the verbal recall onset of each discrete event memory. Hippocampal HFO rate increased roughly 2 s before event recall onset [$n = 12$ participants and $n = 90$ hippocampal contacts; $P = 0.043$, cluster-based permutation test (fig. S7); Hedge's $g = 0.987$, comparing 1-s window before verbal recall onset to matched preonset baseline].

Hippocampal-cortical co-HFOs in brain regions that underlie event segmentation

We next examined the presence of co-HFOs during the stimulus viewing period. Because co-HFOs may coordinate the activity of hippocampal and cortical regions (*21*), we hypothesized that co-HFOs are associated with event segmentation processes during the perception of continuous narratives. Our previous analysis demonstrated an increase in hHFO rate in the 2-s window following event boundaries, so we examined HFOs in the same window for this analysis. Using a data-driven approach, we found that co-HFOs increase after event boundaries in a wide cortical network (Bonferroni-corrected $P < 0.05$; Fig. 3A and figs. S8 and S9). We hypothesized that if co-HFOs are involved in event segmentation, then they should exhibit overlap with cortical regions identified in fMRI studies to subserve this process (*8*, *28*). To quantify this, we isolated the three cortical regions identified by Hahamy *et al.* (*28*) to be involved in event

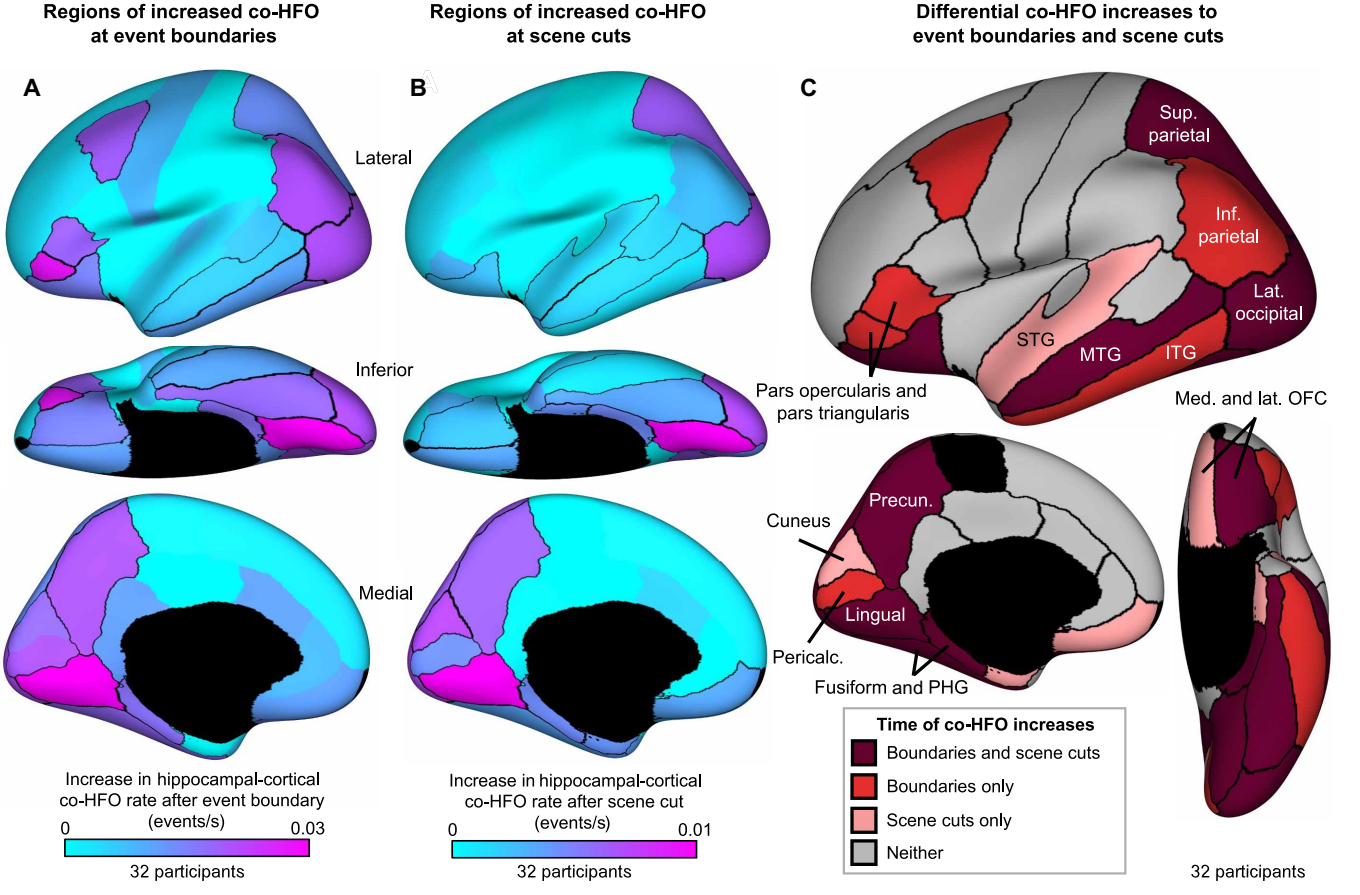

Fig. 3. Hippocampal-cortical co-HFOs increase in an ensemble of higher-order regions. (**A** and **B**) Increase in hippocampal-cortical co-HFOs (A) following $n = 9$ event boundaries (compared to before boundaries) and (B) following $n = 145$ scene cuts (compared to before cuts) averaged over all contacts within each Desikan-Killiany atlas parcel and plotted on a normalized inflated brain (total $n = 32$ participants). Warmer colors indicate greater increases in co-HFO rate. Outlined parcels denote statistical significance at $P < 0.05$ (Bonferroni-corrected, Student's t test). Also see fig. S9, which illustrates the mean and standard error of co-HFO increases following event boundaries and scene cuts for each cortical region. (**C**) Summary plot detailing the location of Desikan-Killiany atlas parcels where contacts exhibited increased hippocampal-cortical co-HFO rate following both event boundaries and scene cuts (dark red), event boundaries only (red), scene cuts only (pink), or neither (gray). Labels are added over selected parcels to aid viewing. ITG, inferior temporal gyrus; MTG, medial temporal gyrus; STG, superior temporal gyrus; OFC, orbitofrontal cortex; PHG, parahippocampal gyrus.

segmentation (angular gyrus, precuneus, and lateral occipital cortex) and identified a significant increase in co-HFOs following event boundaries in these regions (one-sample signed-rank $z = 4.467$, $P < 0.001$, Hedge's $g = 0.508$; fig. S10).

We also found that co-HFOs were increased after event boundaries across both the "higher-order" (including inferior parietal cortex, lateral orbitofrontal cortex, and inferior frontal cortex) and "lower-order" (lingual gyrus, precuneus, and fusiform gyrus) event segmentation cortical regions. To determine whether co-HFOs show specificity based on the granularity of the segmentation level, we performed the same analysis as above using scene cuts (changes in camera angle or view within the continuous narrative; $n = 145$ scene cuts within the viewed clip). Because scene cuts are known to preferentially recruit lower-order visual regions (*32*), we hypothesized that co-HFOs would predominantly increase there. We found that co-HFOs also increase after scene cuts in a wide cortical network, primarily cortical regions involved in visual processing [Bonferroni-corrected $P < 0.05$ (Fig. 3B); mean magnitude of co-HFO increase by cortical parcel is shown in fig. S9]. Increases in co-HFO rate following event boundaries and scene cuts overlap in lower-order visual regions. The regions that exhibit increased co-HFOs after event boundaries but not scene cuts coincide with higher-order event segmentation regions that serve as association cortices (including inferior parietal cortex, inferior frontal cortex, and inferior temporal cortex) (Fig. 3C).

We next aimed to link this finding with recall performance. We isolated cortical regions exhibiting increased co-HFO rate following event boundaries (Fig. 3A). These regions showed higher co-HFO rate following event boundaries for events that were subsequently recalled compared to those that were not (mean value of 0.035 ± 0.001 versus 0.027 ± 0.001 co-HFOs/s; signed-rank $z = 3.884$, $P < 0.001$, Hedge's $g = 0.170$). This relationship was not replicated for cortical regions that exhibited increased co-HFO rate following scene cuts (mean value of 0.030 ± 0.001 versus 0.029 ± 0.001 co-HFOs/s; signed-rank $z = 0.714$, $P = 0.475$, Hedge's $g = 0.009$). Together, co-HFOs occur predominantly in regions that may underlie event segmentation. Furthermore, the magnitude of co-HFOs in higher-order, but not lower-order, event segmentation regions following event boundaries relates to memory performance.

Relation of co-HFO motifs to postboundary replay

The period immediately following an event boundary is thought to contain replay processes for the preceding event (*28*, *30*, *34*). Co-HFOs may serve to synchronize brain regions involved in this process. As the content and memory representations differ across events, co-HFOs may exhibit specificity for each event. In this case, it is possible that the spatial patterns of co-HFOs are similar between event viewing and the immediately following replay period. To investigate this, we calculated a "co-HFO index," or a measure of the consistency in spatial and temporal co-HFO patterns between two epochs (Fig. 4A). This methodology maintains spatial relationships between contacts and controls for variation in baseline co-HFO rates across contact pairs. We calculated this index using every combination of contacts in the hippocampus and cortex, as not all co-HFOs involve the hippocampus and rates of cortico-cortical HFOs may differ by cortical region (fig. S11). We quantified the co-HFO index between event viewing and replay (including both the immediately succeeding replay window and all subsequent replay windows) and between event viewing and recall (Fig. 4, B to D).

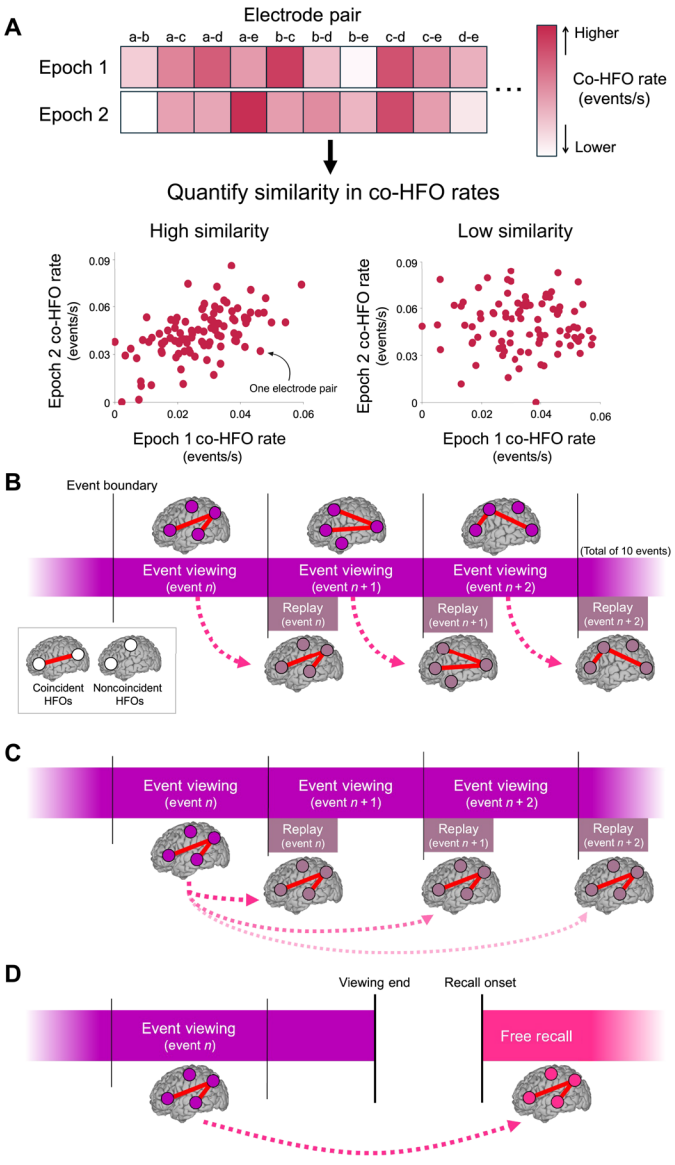

Fig. 4. Hypotheses for co-HFO motifs. (**A**) Schematic describing the quantification of co-HFO motifs across the task paradigm. The magnitude of co-HFO pattern similarity was defined as the Pearson's correlation coefficient of co-HFO rates for every contact pair between any two epochs (e.g., viewing and replay window). Hence, higher correlation coefficients indicate higher co-HFO motif similarity. (**B** to **D**) Tested hypotheses of co-HFO motifs: (B) Co-HFO motifs may reoccur in the window immediately following event boundaries for the immediately preceding viewed event; (C) co-HFO motifs may reoccur in the window immediately following event boundaries for subsequent events; and (D) co-HFO motifs may reoccur during memory retrieval.

We assessed the similarity in co-HFO motifs between event viewing and replay (2-s windows following event boundaries). As we also aimed to assess subsequent replay periods, we normalized the number of events in each group by analyzing only the first five viewed events in each participant. We found high similarity in co-HFO motifs (high co-HFO index) between the event and the immediately following replay window ($P < 0.001$, permutation test; Hedge's g compared to negative lag = 0.377; Fig. 5A). This effect is

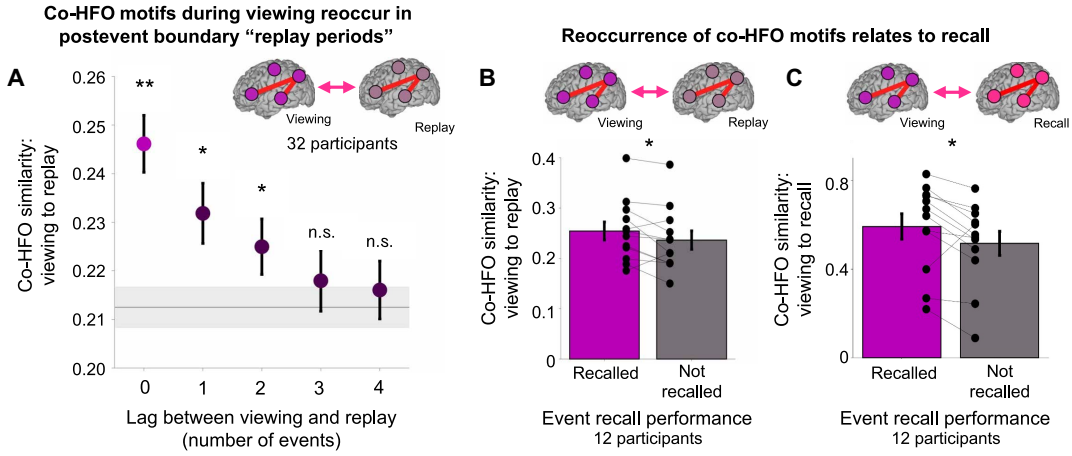

Fig. 5. Co-HFO motifs during viewing reoccur following event boundaries and relate to scene memory. (**A**) Mean similarity in co-HFO patterns for a viewed event and the postevent boundary "replay periods" following the next four events. Only the first five viewed events were used in this analysis ($n = 32$ participants). Pink denotes the similarity between a viewed event and its immediately following postevent boundary replay period. Error bars represent 1 SEM. Gray horizontal line represents mean co-HFO similarity when lags are shuffled, and the shaded area represents 1 bootstrap SEM. $^*P < 0.05$; $^{**}P < 0.01$, permutation test. (**B**) Group-level ($n = 12$ participants) mean co-HFO pattern similarity between event viewing and immediately following replay, averaged across events that were subsequently recalled (magenta) and not recalled (gray). One point represents one unique participant. $^*P < 0.05$, paired-sample t test. (**C**) Group-level mean co-HFO pattern similarity between event viewing and the entire duration of free recall, comparing event viewing for events that were subsequently recalled (magenta) and not recalled (gray). One point represents one unique participant. $^*P < 0.05$, paired-sample t test.

seen in 22 of 32 participants and eight of nine scenes (fig. S12). Furthermore, co-HFO pattern similarity continues to be significant, albeit at lower values, for the next two replay windows ($P = 0.023$ and $P = 0.029$; Hedge's $g = 0.285$ and 0.289, respectively) before diminishing (Fig. 5A). The value for an event-to-replay delay of one scene was compared to a distribution of jittered events (1000 permutation iterations) with fixed event-to-replay durations and was found to be significant ($P < 0.001$). Hence, co-HFO motifs show stability between scene viewing and replay, and these patterns decay as additional events are viewed and replayed. This may provide evidence for how the brain reengages memory traces from previously viewed scenes to encode a present one.

We then assessed the relationship between reoccurrence of co-HFO motifs and recall performance. We first assessed co-HFO similarity between scene viewing and the immediately following replay period and found that scenes that were subsequently recalled exhibited a higher viewing-to-replay period co-HFO index compared to scenes that were not recalled [$t(11) = 2.248$, $P = 0.046$, Hedge's $g = 0.277$; Fig. 5B]. We then replicated this analysis between scene viewing and memory retrieval. The co-HFO index between the recall period and the viewing of recalled events was higher compared to the index between the recall period and viewing of nonrecalled events [mean value of 0.592 ± 0.057 for recalled scenes compared to 0.516 ± 0.054 for nonrecalled scenes; paired $t(11) = 2.638$, $P = 0.023$. Hedge's $g = 0.382$; Fig. 5C]. Hence, specific patterns of co-HFOs occur during encoding that reoccur during replay of the event following event boundaries and again during memory retrieval. Furthermore, the reinstatement of these motifs relates to memory behavior.

Dynamics of hHFOs around participant-level event boundaries

Although the event boundaries that we use in this study exhibited high interparticipant consistency, it is likely that there is some variation in what each participant percieved as an event boundary. To this end, hHFOs may serve as a biomarker for "participant-specific" event boundaries. Because scenes that evoke postviewing replay are linked to improved memory performance and hHFOs are linked with replay processes, we investigated this by examining whether hHFO rate increases following specific scenes (as defined by scene cuts) that were later recalled by participants. We identified that there was no significant increase in hHFO rate relative to all scene cuts (Fig. 6A), but when this analysis was limited to specific scenes that were later recalled, we found that hHFO rate increased 1 to 2 s following the offset of these scenes ($P = 0.048$, cluster-based permutation test jittering HFO events in the same epoch; Hedge's $g = 0.284$; Fig. 6B). This relationship is maintained even after scenes that coincided with an event boundary were removed (8.9% of recalled scenes were within 3 s of an event boundary and were removed; $P = 0.040$; fig. S13).

DISCUSSION

Summary

Experiences from the real world consist of consecutive, oftentimes interdependent, events. To process these events, two processes must occur: (i) segmentation, or chunking, of the continuous stimuli into discrete events at event boundaries and (ii) consolidation of event episodic memory into cortical stores. Co-HFOs represent a potential mechanism by which brain regions coordinate activity (*21*). In this study, we examined the presence of hippocampal and cortical HFOs during the viewing and free recall of a continuous stimulus. We show that co-HFOs in the hippocampus and specific cortical regions increase following event boundaries. The cortical regions that are recruited by co-HFOs are modulated by the granularity of the boundary. Last, the magnitude of activation relates to subsequent memory performance. Hence, HFOs may guide event segmentation processes. Next, specific spatiotemporal patterns of co-HFOs during viewing are found to reoccur in a short window following

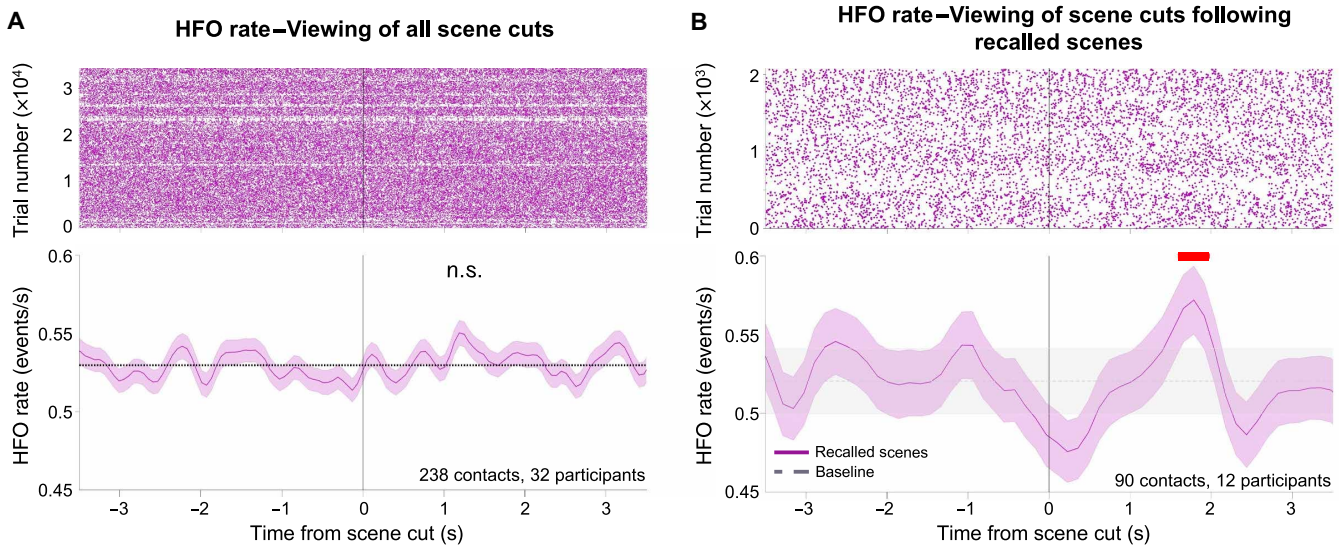

Fig. 6. Hippocampal HFOs mark participant-specific event boundaries. (**A**) Hippocampal HFO rate raster plot and PETH time-locked to scene cuts ($n = 238$ contacts across $n = 32$ participants and $n = 145$ scene cuts). Shaded areas represent 1 bootstrap SEM computed over hHFO events. Dotted line represents the mean hHFO rate over this epoch. n.s., not significant (permutation test compared to shuffled hHFO timings in the same epoch). (**B**) Hippocampal HFO rate raster plot and PETH time-locked to scene cuts following scenes that were recalled ($n = 90$ contacts across $n = 12$ participants). Shaded areas represent 1 bootstrap SEM computed over hHFO events. Dashed line represents the mean hHFO rate over this epoch. Red line indicates significance at $P < 0.05$ (permutation test compared to shuffled hHFO timings in the same epoch).

event boundaries and during event memory retrieval. As these co-HFO motifs continue to persist several events beyond the viewed event, they may serve as a mechanism by which the brain integrates memories from previous events in the processing of subsequent ones. This is also suggestive of HFO-driven replay processes that occur following event boundaries. Together, human HFOs play a substantial, coordinating role in the viewing, processing, and retrieval of continuous narratives.

Defining HFOs

Local field potential activity can be divided into two subgroups: nonoscillatory and oscillatory. Nonoscillatory high-frequency activity (also known as broadband high-frequency activity) is irregular, broad-spectrum signal fluctuations that do not follow a rhythmic pattern and are correlated with multiunit activity (*35*). High-frequency oscillatory phenomena, on the other hand, represent rhythmic and often regular fluctuations in neural excitability that may or may not be associated with ordered neuronal firing (*36*). Coincidence of oscillations across multiple regions may lead to more optimal binding of activity, hence creating circumstances ideal for long-term potentiation (*37*). Two predominant physiological HFOs that are thought to play a prominent role for memory and cognition because they relate to memory-associated neuronal firing are gamma/epsilon and ripple (*36*). Extensive studies in rodents have found that gamma/epsilon oscillations are guided by theta oscillations and predominate memory processing in the wakeful, effortful, and active states. They serve as a means of coordinating memory representations from the hippocampus to the cortex (*36*). Ripple oscillations occur in offline, passive states and serve as a biomarker for event memory replay processes (*38*). However, it is perplexing that recent human studies have identified a role of gamma/epsilon oscillations during memory recall (*39*) and ripple oscillations (including in a wide cortical network) (*20*, *21*, *24*, *40*) during memory encoding (*16*). Furthermore, properties of detected human ripple oscillations (rate, frequency, amplitude, and duration) show stability across task states, including encoding and recall (*41*). Because it is difficult to accurately disentangle different HFOs using human iEEG recordings and HFO subtypes have very similar frequency ranges, it is possible that studies that have assessed HFOs have encompassed multiple subtypes of HFOs. We also cannot rule out that dynamics of gamma/epsilon and ripple oscillations differ in humans (for example, offline and online processes may co-occur in the awake state). Methodological advances in HFO subtype detection may enable us to return and better elucidate the precise contribution of gamma/epsilon and ripple oscillations in our findings. It should also be emphasized that although the term HFO has been used to describe pathological events and epileptic networks (*31*), the HFOs that we report here were detected outside of epileptic networks, and periods of epileptiform activity were excluded. Hence, this is suggestive that these detected HFOs are more representative of physiological activity.

Directionality of influence around of co-HFOs

Co-HFOs may represent a precise means of communication between disparate areas of the brain at event boundaries. However, the directionality of this communication is not well elucidated. Initial human HFO studies examined the influence of hippocampal rippleband HFO-associated activity in task-specific cortical regions (*16*, *17*, *27*, *42*). This aligns with prominent models of memory suggestive of hippocampal-driven influence of memory-containing cortical regions during encoding and recall (*36*, *38*). However, more recent studies have identified a corticocortical pattern of influence (*24*). This may more closely align with theories proposing a potential role of cortical regions in influencing other cortical regions and the hippocampus (*43*). In our study, we found both hippocampal-cortical and corticocortical co-HFO dynamics around time points thought to be relevant for episodic memory function. We also found that, across cortical

regions, 9 to 23% of corticocortical co-HFOs were coincident with an hHFO, even for structures that are thought to be directly connected to the hippocampus. Although we were not able to precisely determine directionality because of the limited spatial and temporal sampling of our technique, future studies should consider the possibility that select cortical regions may be driving synchronized memory network activity (which may be in conjunction with, or independent of, the hippocampus). This may also lend support to the hypothesis that HFOs across the cortical surface serve as a more universal phenomenon that marks interareal information exchange (*44*).

Event segmentation and event boundaries

Event boundaries represent time points where a continuous narrative is segmented into discrete events, a process that is supported by a widespread cortical network (*7*, *11*). This includes earlier hierarchical processing in regions that are more sensitive to sensory changes within the event (such as visual or auditory changes) and higher-level associative regions that are more receptive to complex or abstract changes (*8*, *45*). fMRI and EEG studies have identified these higher-order regions to include the angular gyrus, precuneus, lateral occipital cortex, medial frontal cortex, and superior/middle temporal gyrus (*8*, *9*, *12*, *28*, *45*, *46*). Despite this, a key question remains about how activity in these distributed nodes is coordinated, as the information stored in episodic memory represents a coherent representation integrated across time. It is theorized that this function is coordinated by the hippocampus, as hippocampal activity increases at event boundaries and is predictive of event memory (*12*, *13*, *29*, *30*, *47*), and the hippocampus contains scene cells that are sensitive to event boundaries (*10*). We support a function of the hippocampus in event segmentation by describing a prominent increase in HFO rate of 1 to 2 s following event boundaries. This is similar to the period of hippocampal activation window that reflects replay processes (*8*, *33*). Furthermore, hippocampal-cortical co-HFOs show specificity in location based on the granularity of the event boundary, as co-HFOs occur at higher rates in both lower-level and higher-level event segmentation regions at event boundaries, but only in lower-level visual regions at scene cuts. These findings align closely with fMRI findings (*8*, *28*) and extend our knowledge by providing increased spatial and temporal resolution of the origins of these activity patterns. To extend this, we found that co-HFO rate in higher-order event segmentation regions following event boundaries relates to subsequent recall performance, a relationship that does not extend to lower-order regions. Together, this is supportive of a link between the hippocampus and cortical event segmentation regions that may be guided by HFOs. There are a few characteristics of these findings that warrant further investigation: First, although our hHFO rates are not the highest that have been reported in awake human studies (*16*, *48*), it is higher than what has been reported in several other studies (*49*). It is not known whether differences in HFO rates across participants are physiological or methodological (e.g., due to differences in electrode placement or HFO detection algorithms), but it is possible that engaging, multisensory stimuli with continuous narratives elicit more HFOs than other cognitive tasks. Second, HFOs may display more intricate dynamics at event boundaries, including transient decreases immediately preceding and during event boundaries. This would relate to literature that describes anticipatory inhibition of specific brain areas at event boundaries (*50*). Although this was not a statistically significant trend in our study, it warrants additional investigation in larger cohorts of participants and contacts.

Subsets of hHFOs

We leveraged this large dataset to examine specific hippocampal regions that may be more involved in coordinating activity associated with event segmentation. Specifically, we aimed to elucidate whether there were differences due to longitudinal axis, hippocampal subfield, or hemispheric laterality, as these were factors used by Norman *et al.* (*17*) when highlighting left-anterior hippocampal contacts within the CA1 to be most associated with autobiographical memory reactivation. Here, we show that contacts in the right-anterior hippocampus and within the CA1 subfield exhibit an increase in activity at event boundaries. The hippocampal CA1 subfield is thought to play a key role in a variety of memory processes and has been shown in rodent literature to display the precise timing and spatial organization required for selective processing and replay of specific memories (*38*, *51*). Furthermore, hHFO events from other hippocampal subfields, such as the CA3 or dentate gyrus, do not have the same impact as the CA1 on hippocampal-cortical communication or on memory performance (*52*–*55*). Our other findings relate to studies that indicate a specific function of the right-anterior hippocampus in the longitudinal integration of memory, specifically in the utilization of prior event memories for the encoding of current, novel ones (*56*, *57*). However, this contrasts with studies that describe a greater role of the posterior hippocampus at event boundaries (*58*). To reconcile this, it is possible that anterior hHFOs implement differing cortical connectivity profiles when coordinating hippocampal-cortical activation (*59*). Furthermore, because the timescale of hippocampal integration differs along the length of the hippocampal axis (with the anterior hippocampus integrating information along a longer timescale) (*60*, *61*), the mechanisms underlying posterior hippocampal fMRI activation at event boundaries may differ in function from increases in anterior hHFOs. It is also possible that HFO rate does not directly reflect increased engagement of cortical regions or networks, either because there is a basal level of HFO activity to support these functions or there are HFO subtypes that exhibit different functions (similar to ongoing studies investigating human theta oscillations) (*62*).

Co-HFO index and pattern reactivation

It is thought that a rapid reactivation of event memory traces occurs at event boundaries, which functions to aid memory consolidation (*63*). This process is also associated with hippocampal activation (*2*, *8*, *13*). Furthermore, several studies have found matching EEG (*29*, *30*) and fMRI (*28*) patterns of neural activity during event viewing and replay periods. Last, hippocampal activation patterns appear to be unique for event memories of different types (*64*). As the location and timing of co-HFOs may index specific firing patterns that encode specific memory representations (*19*, *65*), we aimed to investigate whether spatial and temporal patterns of co-HFOs index event memory and whether these motifs reoccur following event viewing. We found that co-HFO motifs during event viewing are unique and show similarity to the postevent replay window (2 s following the terminating event boundary). The magnitude of co-HFO index between viewing and replay relates to subsequent event memory performance. Last, these same motifs arise again during memory recall. This is indicative that co-HFOs across the hippocampal-cortical memory network contain event-specific representations. Co-HFO motifs may drive initial memory encoding during event viewing and reactivate the same regions during postevent boundary replay periods and during retrieval of event memory. One interesting caveat to

this approach is that it is possible that specific events engage a particular sensory modality more than others, which would affect the magnitude of primary cortex co-HFO during scene viewing (e.g., a scene with vivid visual stimuli better engages the visual system during replay but not the auditory or language processing systems). To this end, it is difficult to distinguish the process of event perception, event segmentation, and memory processing; furthermore, the extent to which primary sensory cortices contain memory representations is not well known (*66*). However, it is likely that these processes are intertwined, such that HFOs will reactivate the same regions that were initially activated during stimulus presentation (*16*, *27*).

It is thought that replay processes following event boundaries contain representations for both the immediately preceding event and several previous events (*11*, *28*, *67*–*69*). This may contribute to a memory scaffold that transcends several event boundaries and binds events longitudinally. This would be key for memory of continuous narratives, as, despite engaging with events only once, there is an inherent narrative that may be followed and re-referenced (e.g., reappearance of a cue from a prior event). We aimed to investigate whether co-HFO motifs persist beyond the current event and are re-referenced in future replay periods. We found that event-specific motifs remain for three subsequent events. As scenes became more temporally distant, co-HFO motif similarity also decreased. This provides evidence for the reactivation of event memory from prior events for the integration of a current event into episodic memory and that this process is facilitated by co-HFOs across the hippocampal-cortical network. This speaks against co-HFOs serving as a continuous scaffolding mechanism by which integrative encoding during stimulus viewing occurs (*70*), as the reoccurrence of co-HFO motifs for a given event diminishes across time. However, we cannot rule out that this process instead occurs in the offline periods following the end of the entire stimulus or that it is driven by a different mechanism.

Participant-specific event boundaries

We also extended our knowledge of event segmentation to "participant-specific event boundaries." Thus far, studies have used event boundaries that have a high interparticipant consistency (*71*), including this study. Although there is some objectivity in this approach of assigning event boundaries, it inherently leads to potential interparticipant variation. Although this variation may be mitigated by large datasets, there is also value in assessing these differences. Here, we assessed whether hHFOs may serve as a biomarker for participant-level event boundaries. The rationale for this was based on prior studies that identified scene chunks associated with event segmentation to be better encoded and have a higher likelihood of being subsequently recalled (*72*, *73*). To investigate this, we divided the stimuli into more granular segments using scene cuts (as they have clear onset and offsets) and found increases in an hHFO rate of 1 to 2 s following scene cut offset for scenes that were later recalled but not for scenes that were not later recalled. This relationship is maintained even after the removal of scene cuts that coincide with event boundaries. Hence, it is possible that hHFOs are an electrophysiological marker for participant-specific event boundaries. Future studies should further investigate discrepancies between population-level and participant-specific event boundaries, including assessing whether the delay between the end of an event or scene and the subsequent increase in HFO rates are different between event boundaries and scene cuts. This may suggest HFO-driven markers for participant-specific processing of continuous narratives.

In conclusion, hippocampal-cortical co-HFOs may enable the brain to process and store continuous narratives by coordinating the networks underlying event segmentation and episodic memory processing. Event-specific spatiotemporal patterns of co-HFOs exist during scene viewing that are replayed immediately following event boundaries and again during retrieval of scene memory. Hence, HFOs represent a robust mechanism that drives the encoding and retrieval of rich, continuous episodic memories from our everyday lives.

METHODS

Participants

Intracranial recordings were obtained from 30 patients (14 females; 32 testing sessions) with medically intractable epilepsy undergoing iEEG recording at Northwell Health (NY, USA) to identify epileptogenic zones for potential surgical treatment (table S1). Data from a subset of these participants ($n = 23$) were used in a previous study (*32*). These patients are continuously monitored with intracranial contacts that were stereotactically placed, subdural grid or strip contacts, or both, for a period of up to 4 weeks. During this time, they may participate in cognitive and functional testing. The decision to implant, the location of implanted contacts, and the duration of implantation were made exclusively on clinical grounds by the clinical treatment team. Participants were invited to participate in this study if their iEEG recording included a hippocampal contact and ability to maintain attention to the 10-min audiovisual stimuli task. This study was conducted in accordance with the Institutional Review Board at the Feinstein Institutes for Medical Research (Northwell Health), and informed consent was obtained before research testing. No clinical seizures occurred during or within the 2-hour period before the experimental block. All participants performed the task in English.

Stimuli and task

Psychophysics Toolbox (version 2014-10-19_V3, GStreamer version 1.10.2) (*74*) running on MATLAB R2012b (MathWorks, Natick, MA, USA) was used for precise stimulus presentation. Patients viewed 600 s of the animated feature film Despicable Me without any explicit memory instruction. The audiovisual clip was presented continuously. Nentwich *et al.* (*32*) previously identified 9 event boundaries and 145 scene cuts (a change in viewing angle or scene; mean intercut interval of 4.6 s) in this clip, which we used for analysis. We also implemented nine scenes that were matched (audio and visual) to event boundaries to control for any inherent properties of event boundaries (e.g., changes in attention or movement) that may affect analysis.

Immediately following viewing, participants were verbally asked to "describe, in as many details as you can, as many things as you can recall from the movie." Participants verbally indicated when they were finished with their recall. The verbal responses were recorded by a microphone affixed to a nearby stable surface for further assessment and quantification in offline analysis. The onsets, offsets, and content of each recall were extracted in an offline analysis using the Audacity auditory presentation software (Audacity, Oak Park, MI, USA). This included the onset of recall for each unique event memory representation or specific, differing aspect of an event. For each viewed scene (as segmented using scene cuts), it was identified whether the participant recalled the scene during recall. Because participants varied in the number of contacts and recall performance, all analyses relating

electrophysiological activity during encoding to memory performance were performed on the group level ($n = 12$ participants).

Intracranial recordings

Intracranial recording sites were stereoelectroencephalography depth electrodes, subdural grids, and/or subdural strips (Ad-Tech Medical Instrument Corp., Oak Creek, WI, USA; Integra LifeSciences, Princeton, NJ, USA; PMT Corp., Chanhassen, MN, USA). Subdural grid/strip contacts were 3-mm platinum disks with 10-mm intercontact spacing. Depth electrode contacts were 2-mm cylinders with 0.8-mm diameter and 4.4- or 2.2-mm intercontact spacing. During the recordings, the intracranial electrode signal was referenced to a subdermal electrode or subdural strip. Neural signals were acquired using a Tucker-Davis Technologies PZ5M module (Tucker-Davis Technologies Inc., Alachua, FL, USA) at 500 Hz, 1.5 kHz, or 3 kHz. During the task, transistor-transistor logic pulses were used to align the onset and offset of the audiovisual clip to synchronize stimulus presentation with neural data.

Data analysis was performed in MATLAB R2023b using FieldTrip (*75*) and custom analysis scripts. Data were resampled to 500 Hz. Power-line noise was removed using a notch filter (zero-lag, linear-phase Hanning-window finite impulse response band-stop filter) at 60, 120, and 180 Hz. Raw iEEG data were inspected visually to detect noisy or bad channels, which were removed from all subsequent analysis. Channels that were identified as being within the seizure onset zone were excluded from analysis. Data were average referenced to remove global artifact.

As study participants underwent clinical care alongside research testing, we implemented notes derived from clinical iEEG review (performed or supervised by S.B.) to exclude all contacts that exhibited any electrophysiological signs of epileptic pathology. This included contacts that exhibited interictal epileptic discharges (IEDs) or were closely related to epileptic foci.

Hippocampal and cortical contact localization

Before electrode implantation, a T1-weighted MRI scan was performed. After implantation, a computed tomography (CT) scan was performed. We used the iELVis toolbox (*76*), BioImage Suite (*77*), and FreeSurfer (*78*) for intracranial electrode localization. Briefly, electrodes were manually registered to the postimplantation CT scan using BioImage Suite, which was coregistered to the preimplantation MRI scan. These images were converted to a standard coordinate space, the cortical and hippocampal fields were segmented, and anatomical locations for each segment was assigned. Last, contact locations were projected onto the standardized brain space. For all anatomical region of interest analysis, these parcellations were used to select contacts of interest.

Hippocampal and cortical HFO detection

HFO detection was performed similar to prior studies (*27*) and with close consideration of established protocols for HFO detection (*49*). The following procedure was repeated for each contact.

For each hippocampal and cortical contact, the signal was bipolar referenced to a nearby white matter contact, defined as a contact containing a proximal tissue density value of less than −0.9 (*79*). This aimed to optimize signal by reducing noise. The resulting rereferenced signal was filtered between 80 and 140 Hz using a zero-lag, linear-phase Hanning-window finite impulse response filter (5-Hz transition band). A Hilbert transform was used to attain HFO-band power envelope. The signal was clipped to 3 SDs and then squared and smoothed using a Kaiser-window finite impulse response low-pass filter with a 40-Hz cutoff. The mean and SD of the entire audiovisual clip period was implemented to attain a baseline for event detection. Events from the power envelope that exceeded 3 SDs above baseline were selected as potential HFO events. The onset and offset of each event were defined as the time points where the 80- to 140-Hz power decreased below 2 SDs above baseline. Events shorter than 21 ms (computed as duration of 3 cycles of 140 Hz) and longer than 250 ms were removed. Events where the peak-to-peak duration was under 200 ms were merged. The HFO peak was then aligned to the nearest maxima of the bipolar-referenced trace. To control for artifacts, a control detection was executed on the common average signal of all contacts. Any HFO events that occurred within 50 ms of a common-average 80- to 140-Hz peak were removed. As pathologic discharge events (IEDs) may appear similar to HFOs, we implemented a stringent automated detection process for their removal. Each bipolar-referenced trace was filtered between 25 and 60 Hz (using a zero-lag, linear-phase Hanning-window finite impulse recovery filter), and a similar methodology to the above was implemented (Hilbert transform, square, and normalize). Detected events that exceeded 5 SDs were marked as IEDs, and all HFO events occurring within 200 ms of these events were excluded. To confirm that all detected HFOs were oscillatory, we implemented the Extended Better Oscillation Detection (eBOSC) toolbox (*80*) and confirmed that each HFO event had at least one oscillatory cycle within the 80- to 140-Hz frequency range. HFO duration (onset-to-offset) and HFO amplitude (from the bipolar-referenced trace) were then extracted. HFO peak frequency was quantified by identifying the frequency with the highest baseline-corrected power across a 100-ms window around the peak of the HFO (using a wavelet with filter order of 6, 1-Hz frequency resolution, and 5-ms temporal resolution). We made the decision to merge putative HFO events with a peak-to-peak interval of less than 200 ms because it is difficult to determine the precise onset and offset of each HFO event. This may contribute to HFOs that appear to be of longer duration. The main findings of this study (Figs. 2A and 5A) were still supported when we instead used HFO events that were detected using parameters used by Norman *et al.* (*16*). This supports the robustness of our findings across detection algorithms.

Perievent time histograms

To construct PETHs of HFO rates locked to specific time points of interest, we identified and used a bin width advised by Scott's optimization method, which optimizes histogram bin size to event density (*81*). We implemented three- or four-point smoothing to aid in visualization. For hHFO rate following event boundaries (Fig. 2A) and following scene cuts (Fig. 6), we used a bin size of 130 ms with a three-point smoothing window. To determine significant time bins, 2000 iterations of PETHs were computed by circularly jittering HFO times across the entire perievent epoch of interest. Cluster-based permutation tests were implemented to determine the time bins with significant increase in HFO rate.

Co-HFO events

A co-HFO event was defined as two HFO events where the peak-to-peak duration was less than 100 ms (defined as half of the maximum 200-ms duration). This was selected because HFO peaks are more readily detectable than the onset and offset. Rates of coincidence

were calculated between the hippocampus and all cortical sites and between each pair of cortical sites. Changes in the rate, for example, around event boundaries or scene cuts, were calculated in coincident events per second.

Quantification of co-HFO motifs

We next aimed to quantify similarity in co-HFOs across the entire brain (all contacts) during encoding, replay, and retrieval. Hence, we developed a methodology that enabled quantification of co-HFO similarity between any two time periods using the rate of co-HFOs in each epoch. Notably, this methodology maintains spatial relationships between contacts, is specific for each event (or time window), and mitigates any baseline co-HFO differences between contact pairs.

We quantify the co-HFO index for each participant. For each contact pair within this participant, we quantify the rate of co-HFOs for each time window of interest. For each epoch of interest, we get a vector where each contact pair contributes one value. Then, for any given two time epochs, we perform a correlation between these vectors. The resulting correlation coefficient is the co-HFO index. In this way, a high co-HFO index indicates that the magnitude of co-HFOs was more similar between the two epochs of interest, and a low co-HFO index indicates that the magnitude of co-HFOs was less similar between the two time windows. Critically, this approach does not necessarily evaluate the contribution of co-HFOs between any two given contact pairs but rather uses a "whole brain" perspective where HFOs are relatively ubiquitous across the cortex and fluctuate in rates and coincidence. The significance of the derived co-HFO index values were calculated using a permutation test where the HFO timings of co-HFOs were jittered in the analysis window.

To ensure that the witnessed effects were not driven by any specific contact pair or pairs of regions, we then computed co-HFO indices between scene viewing and the immediately following replay window where one pair of contacts was removed from analysis. The change in co-HFO index value was taken to reflect the magnitude of effect that this pair of contacts had on this analysis. We then repeated this process for all contact pairs. To visualize these data, we created a matrix where the magnitude of effect for contacts in each pair of cortical parcels was plotted. We did not identify any regions that visually appear to make a substantial impact on the co-HFO index.

General linear model

A general linear model was used to investigate specific properties of contacts that contributed most to the increase in HFO rate following event boundaries. The variables selected for analysis (contact in CA1 versus not, contact in anterior versus posterior hippocampus, and left versus right hemisphere) were selected on the basis of a prior study that used the same factors (*17*). We assessed the impact of each factor and all interaction effects on the magnitude of increase in HFO rate following event boundaries. This normalized our analysis to account for any variation in baseline HFO rate across contacts. To assess for significance, we generated a permutation distribution for the β value of each factor and interaction effect by shuffling contact labels 2000 times and recalculating the model for each iteration. To confirm that the effects depicted in our analysis are also seen on a nonmodeled dataset, we also depict the increase in HFO rate following event boundaries by hemisphere and longitudinal position (Fig. 2).

$$\begin{aligned}\text{HFO rate increase} \sim\ & \text{CA1} + \text{LongitudinalPosition} \\ & + \text{Hemisphere} + \text{CA1} \times \text{LongitudinalPosition} \\ & + \text{CA1} \times \text{Hemisphere} \\ & + \text{LongitudinalPosition} \times \text{Hemisphere} \\ & + \text{CA1} \times \text{LongitudinalPosition} \times \text{Hemisphere}\end{aligned}$$

Statistical testing

Two-tailed tests were used for all statistical testing, a P value of 0.05 was used to determine statistical significance, and a P value of 0.10 was used to identify potential trends in the data. All means are reported alongside SEM, unless otherwise stated. Effect sizes are reported using Hedge's g. Effect sizes for event rates were calculated across participants comparing a 1-s window (starting 1 s following to event boundary or scene cut or 2 s before verbal recall onset) to a matched-duration, baseline window (starting 3 s before event boundary, scene cut, or recall).

Supplementary Materials

This PDF file includes:

Figs. S1 to S13
Tables S1 and S2

REFERENCES AND NOTES

1. J. M. Zacks, N. K. Speer, K. M. Swallow, T. S. Braver, J. R. Reynolds, Event perception: A mind–brain perspective. *Psychol. Bull.* **133**, 273–293 (2007).
2. Z. M. Reagh, C. Ranganath, Flexible reuse of cortico-hippocampal representations during encoding and recall of naturalistic events. *Nat. Commun.* **14**, 1279 (2023).
3. M. T. Kucewicz, G. A. Worrell, N. Axmacher, Direct electrical brain stimulation of human memory: Lessons learnt and future perspectives. *Brain* **146**, 2214–2226 (2023).
4. H. Eichenbaum, A cortical–hippocampal system for declarative memory. *Nat. Rev. Neurosci.* **1**, 41–50 (2000).
5. T. J. Teyler, P. DiScenna, The hippocampal memory indexing theory. *Behav. Neurosci.* **100**, 147–154 (1986).
6. K. M. Swallow, J. M. Zacks, Sequences learned without awareness can orient attention during the perception of human activity. *Psychon. Bull. Rev.* **15**, 116–122 (2008).
7. G. A. Radvansky, J. M. Zacks, Event boundaries in memory and cognition. *Curr. Opin. Behav. Sci.* **17**, 133–140 (2017).
8. C. Baldassano, J. Chen, A. Zadbood, J. W. Pillow, U. Hasson, K. A. Norman, Discovering event structure in continuous narrative perception and memory. *Neuron* **95**, 709–721. e5 (2017).
9. N. K. Speer, J. M. Zacks, J. R. Reynolds, Human brain activity time-locked to narrative event boundaries. *Psychol. Sci.* **18**, 449–455 (2007).
10. J. Zheng, A. G. P. Schjetnan, M. Yebra, B. A. Gomes, C. P. Mosher, S. K. Kalia, T. A. Valiante, A. N. Mamelak, G. Kreiman, U. Rutishauser, Neurons detect cognitive boundaries to structure episodic memories in humans. *Nat. Neurosci.* **25**, 358–368 (2022).
11. B. J. Griffiths, L. Fuentemilla, Event conjunction: How the hippocampus integrates episodic memories across event boundaries. *Hippocampus* **30**, 162–171 (2020).
12. A. Ben-Yakov, Y. Dudai, Constructing realistic engrams: Poststimulus activity of hippocampus and dorsal striatum predicts subsequent episodic memory. *J. Neurosci.* **31**, 9032–9042 (2011).
13. A. Ben-Yakov, R. N. Henson, The hippocampal film editor: Sensitivity and specificity to event boundaries in continuous experience. *J. Neurosci.* **38**, 10057–10068 (2018).
14. M. Silva, X. Wu, M. Sabio, E. Conde-Blanco, P. Roldan, A. Donaire, M. Carreño, N. Axmacher, C. Baldassano, L. Fuentemilla, Movie-watching evokes ripple-like activity within events and at event boundaries. *Nat. Commun.* **16**, 5647 (2025).
15. M. F. Carr, S. P. Jadhav, L. M. Frank, Hippocampal replay in the awake state: A potential substrate for memory consolidation and retrieval. *Nat. Neurosci.* **14**, 147–153 (2011).
16. Y. Norman, E. M. Yeagle, S. Khuvis, M. Harel, A. D. Mehta, R. Malach, Hippocampal sharp-wave ripples linked to visual episodic recollection in humans. *Science* **365**, eaax1030 (2019).
17. Y. Norman, O. Raccah, S. Liu, J. Parvizi, R. Malach, Hippocampal ripples and their coordinated dialogue with the default mode network during recent and remote recollection. *Neuron* **109**, 2767–2780.e5 (2021).

18. A. P. Vaz, S. K. Inati, N. Brunel, K. A. Zaghloul, Coupled ripple oscillations between the medial temporal lobe and neocortex retrieve human memory. *Science* **363**, 975–978 (2019).
19. A. P. Vaz, J. H. Wittig Jr., S. K. Inati, K. A. Zaghloul, Replay of cortical spiking sequences during human memory retrieval. *Science* **367**, 1131–1134 (2020).
20. C. W. Dickey, I. A. Verzhbinsky, X. Jiang, B. Q. Rosen, S. Kajfez, E. N. Eskandar, J. Gonzalez-Martinez, S. S. Cash, E. Halgren, Cortical ripples during NREM sleep and waking in humans. *J. Neurosci.* **42**, 7931–7946 (2022).
21. C. W. Dickey, I. A. Verzhbinsky, X. Jiang, B. Q. Rosen, S. Kajfez, B. Stedelin, J. J. Shih, S. Ben-Haim, A. M. Raslan, E. N. Eskandar, J. Gonzalez-Martinez, S. S. Cash, E. Halgren, Widespread ripples synchronize human cortical activity during sleep, waking, and memory recall. *Proc. Natl. Acad. Sci. U.S.A.* **119**, e2107797119 (2022).
22. H. R. Joo, L. M. Frank, The hippocampal sharp wave–ripple in memory retrieval for immediate use and consolidation. *Nat. Rev. Neurosci.* **19**, 744–757 (2018).
23. Y. Liu, R. J. Dolan, Z. Kurth-Nelson, T. E. J. Behrens, Human replay spontaneously reorganizes experience. *Cell* **178**, 640–652.e14 (2019).
24. I. A. Verzhbinsky, D. B. Rubin, S. Kajfez, Y. Bu, J. N. Kelemen, A. Kapitonava, Z. M. Williams, L. R. Hochberg, S. S. Cash, E. Halgren, Co-occurring ripple oscillations facilitate neuronal interactions between cortical locations in humans. *Proc. Natl. Acad. Sci. U.S.A.* **121**, e2312204121 (2024).
25. S. McKenzie, N. Nitzan, D. F. English, Mechanisms of neural organization and rhythmogenesis during hippocampal and cortical ripples. *Philos. Trans. R. Soc. B* **375**, 20190237 (2020).
26. D. Khodagholy, J. N. Gelinas, G. Buzsáki, Learning-enhanced coupling between ripple oscillations in association cortices and hippocampus. *Science* **358**, 369–372 (2017).
27. A. Mishra, S. Akkol, E. Espinal, N. Markowitz, G. Tostaeva, E. Freund, A. D. Mehta, S. Bickel, Hippocampal and cortical high-frequency oscillations orchestrate human semantic networks during word list memory. *iScience* **28**, 112171 (2025).
28. A. Hahamy, H. Dubossarsky, T. E. J. Behrens, The human brain reactivates context-specific past information at event boundaries of naturalistic experiences. *Nat. Neurosci.* **26**, 1080–1089 (2023).
29. M. Silva, C. Baldassano, L. Fuentemilla, Rapid memory reactivation at movie event boundaries promotes episodic encoding. *J. Neurosci.* **39**, 8538–8548 (2019).
30. I. Sols, S. DuBrow, L. Davachi, L. Fuentemilla, Event boundaries trigger rapid memory reinstatement of the prior events to promote their representation in long-term memory. *Curr. Biol.* **27**, 3499–3504.e4 (2017).
31. M. T. Kucewicz, J. Cimbalnik, J. S. S. Garcia, M. Brazdil, G. A. Worrell, High frequency oscillations in human memory and cognition: A neurophysiological substrate of engrams? *Brain* **147**, 2966–2982 (2024).
32. M. Nentwich, M. Leszczynski, B. E. Russ, L. Hirsch, N. Markowitz, K. Sapru, C. E. Schroeder, A. D. Mehta, S. Bickel, L. C. Parra, Semantic novelty modulates neural responses to visual change across the human brain. *Nat. Commun.* **14**, 2910 (2023).
33. D. K. Bilkey, C. Jensen, Neural markers of event boundaries. *Top. Cogn. Sci.* **13**, 128–141 (2021).
34. S. Michelmann, U. Hasson, K. A. Norman, Evidence that event boundaries are access points for memory retrieval. *Psychol. Sci.* **34**, 326–344 (2022).
35. M. Leszczyński, A. Barczak, Y. Kajikawa, I. Ulbert, A. Y. Falchier, I. Tal, S. Haegens, L. Melloni, R. T. Knight, C. E. Schroeder, Dissociation of broadband high-frequency activity and neuronal firing in the neocortex. *Sci. Adv.* **6**, eabb0977 (2020).
36. G. Buzsáki, F. L. da Silva, High frequency oscillations in the intact brain. *Prog. Neurobiol.* **98**, 241–249 (2012).
37. B. J. Griffiths, O. Jensen, Gamma oscillations and episodic memory. *Trends Neurosci.* **46**, 832–846 (2023).
38. G. Buzsáki, Hippocampal sharp wave-ripple: A cognitive biomarker for episodic memory and planning. *Hippocampus* **25**, 1073–1188 (2015).
39. D. Osipova, A. Takashima, R. Oostenveld, G. Fernández, E. Maris, O. Jensen, Theta and gamma oscillations predict encoding and retrieval of declarative memory. *J. Neurosci.* **26**, 7523–7531 (2006).
40. J. C. Garrett, I. A. Verzhbinsky, E. Kaestner, C. Carlson, W. K. Doyle, O. Devinsky, T. Thesen, E. Halgren, Binding of cortical functional modules by synchronous high-frequency oscillations. *Nat. Hum. Behav.* **8**, 1988–2002 (2024).
41. Y. Y. Chen, L. Aponik-Gremillion, E. Bartoli, D. Yoshor, S. A. Sheth, B. L. Foster, Stability of ripple events during task engagement in human hippocampus. *Cell Rep.* **35**, 109304 (2021).
42. S. Henin, A. Shankar, H. Borges, A. Flinker, W. Doyle, D. Friedman, O. Devinsky, G. Buzsáki, A. Liu, Spatiotemporal dynamics between interictal epileptiform discharges and ripples during associative memory processing. *Brain* **144**, 1590–1602 (2021).
43. K. Kaefer, F. Stella, B. L. McNaughton, F. P. Battaglia, Replay, the default mode network and the cascaded memory systems model. *Nat. Rev. Neurosci.* **23**, 628–640 (2022).
44. S. Prathapagiri, J. Cimbalnik, J. S. G. Salinas, M. Galanina, L. Jurkovicova, P. Daniel, M. Kojan, R. Roman, M. Pail, W. Fortuna, M. Sluzewska-Niedzwiedz, P. Tabakow, A. Czyzewski, M. Brazdil, M. T. Kucewicz, Coincident bursts of high frequency oscillations across the human cortex coordinate large-scale memory processing. bioRxiv 644989 [Preprint] (2025). https://doi.org/10.1101/2025.03.24.644989.
45. J. M. Zacks, T. S. Braver, M. A. Sheridan, D. I. Donaldson, A. Z. Snyder, J. M. Ollinger, R. L. Buckner, M. E. Raichle, Human brain activity time-locked to perceptual event boundaries. *Nat. Neurosci.* **4**, 651–655 (2001).
46. S. DuBrow, L. Davachi, Temporal binding within and across events. *Neurobiol. Learn. Mem.* **134**, 107–114 (2016).
47. A. J. Barnett, M. Nguyen, J. Spargo, R. Yadav, B. I. Cohn-Sheehy, C. Ranganath, Hippocampal-cortical interactions during event boundaries support retention of complex narrative events. *Neuron* **112**, 319–330.e7 (2024).
48. H. Zhang, I. Skelin, S. Ma, M. Paff, L. Mnatsakanyan, M. A. Yassa, R. T. Knight, J. J. Lin, Awake ripples enhance emotional memory encoding in the human brain. *Nat. Commun.* **15**, 215 (2024).
49. A. A. Liu, S. Henin, S. Abbaspoor, A. Bragin, E. A. Buffalo, J. S. Farrell, D. J. Foster, L. M. Frank, T. Gedankien, J. Gotman, J. A. Guidera, K. L. Hoffman, J. Jacobs, M. J. Kahana, L. Li, Z. Liao, J. J. Lin, A. Losonczy, R. Malach, M. A. van der Meer, K. McClain, B. L. McNaughton, Y. Norman, A. Navas-Olive, L. M. de la Prida, J. W. Rueckemann, J. J. Sakon, I. Skelin, I. Soltesz, B. P. Staresina, S. A. Weiss, M. A. Wilson, K. A. Zaghloul, M. Zugaro, G. Buzsáki, A consensus statement on detection of hippocampal sharp wave ripples and differentiation from other fast oscillations. *Nat. Commun.* **13**, 6000 (2022).
50. C. S. Lee, M. Aly, C. Baldassano, Anticipation of temporally structured events in the brain. *eLife* **10**, e64972 (2021).
51. G. Girardeau, M. Zugaro, Hippocampal ripples and memory consolidation. *Curr. Opin. Neurobiol.* **21**, 452–459 (2011).
52. I. Lee, G. Rao, J. J. Knierim, A double dissociation between hippocampal subfields differential time course of CA3 and CA1 place cells for processing changed environments. *Neuron* **42**, 803–815 (2004).
53. J. Stokes, C. Kyle, A. D. Ekstrom, Complementary roles of human hippocampal subfields in differentiation and integration of spatial context. *J. Cogn. Neurosci.* **27**, 546–559 (2015).
54. H. R. Dimsdale-Zucker, M. Ritchey, A. D. Ekstrom, A. P. Yonelinas, C. Ranganath, CA1 and CA3 differentially support spontaneous retrieval of episodic contexts within human hippocampal subfields. *Nat. Commun.* **9**, 294 (2018).
55. J. J. Sakon, M. J. Kahana, Hippocampal ripples signal contextually mediated episodic recall. *Proc. Natl. Acad. Sci. U.S.A.* **119**, e2201657119 (2022).
56. E. F. Chua, D. L. Schacter, E. Rand-Giovannetti, R. A. Sperling, Evidence for a specific role of the anterior hippocampal region in successful associative encoding. *Hippocampus* **17**, 1071–1080 (2007).
57. M. L. Schlichting, J. A. Mumford, A. R. Preston, Learning-related representational changes reveal dissociable integration and separation signatures in the hippocampus and prefrontal cortex. *Nat. Commun.* **6**, 8151 (2015).
58. Z. M. Reagh, A. I. Delarazan, A. Garber, C. Ranganath, Aging alters neural activity at event boundaries in the hippocampus and posterior medial network. *Nat. Commun.* **11**, 3980 (2020).
59. L. Tang, P. J. Pruitt, Q. Yu, R. Homayouni, A. M. Daugherty, J. S. Damoiseaux, N. Ofen, Differential functional connectivity in anterior and posterior hippocampus supporting the development of memory formation. *Front. Hum. Neurosci.* **14**, 204 (2020).
60. I. K. Brunec, B. Bellana, J. D. Ozubko, V. Man, J. Robin, Z.-X. Liu, C. Grady, R. S. Rosenbaum, G. Winocur, M. D. Barense, M. Moscovitch, Multiple scales of representation along the hippocampal anteroposterior axis in humans. *Curr. Biol.* **28**, 2129–2135.e6 (2018).
61. K. D. Duncan, M. L. Schlichting, Hippocampal representations as a function of time, subregion, and brain state. *Neurobiol. Learn. Mem.* **153**, 40–56 (2018).
62. A. Goyal, J. Miller, S. E. Qasim, A. J. Watrous, H. Zhang, J. M. Stein, C. S. Inman, R. E. Gross, J. T. Willie, B. Lega, J.-J. Lin, A. Sharan, C. Wu, M. R. Sperling, S. A. Sheth, G. M. McKhann, E. H. Smith, C. Schevon, J. Jacobs, Functionally distinct high and low theta oscillations in the human hippocampus. *Nat. Commun.* **11**, 2469 (2020).
63. B. E. Pfeiffer, The content of hippocampal "replay". *Hippocampus* **30**, 6–18 (2020).
64. B. Milivojevic, M. Varadinov, A. V. Grabovetsky, S. H. P. Collin, C. F. Doeller, Coding of event nodes and narrative context in the hippocampus. *J. Neurosci.* **36**, 12412–12424 (2016).
65. A. P. S. Tong, A. P. Vaz, J. H. Wittig, S. K. Inati, K. A. Zaghloul, Ripples reflect a spectrum of synchronous spiking activity in human anterior temporal lobe. *eLife* **10**, e68401 (2021).
66. L. Muckli, L. S. Petro, The significance of memory in sensory cortex. *Trends Neurosci.* **40**, 255–256 (2017).
67. C. H. C. Chang, S. A. Nastase, U. Hasson, Information flow across the cortical timescale hierarchy during narrative construction. *Proc. Natl. Acad. Sci. U.S.A.* **119**, e2209307119 (2022).
68. B. I. Cohn-Sheehy, A. I. Delarazan, Z. M. Reagh, J. E. Crivelli-Decker, K. Kim, A. J. Barnett, J. M. Zacks, C. Ranganath, The hippocampus constructs narrative memories across distant events. *Curr. Biol.* **31**, 4935–4945.e7 (2021).
69. D. Clewett, S. DuBrow, L. Davachi, Transcending time in the brain: How event memories are constructed from experience. *Hippocampus* **29**, 162–183 (2019).
70. L. Nadel, A. Hupbach, R. Gomez, K. Newman-Smith, Memory formation, consolidation and transformation. *Neurosci. Biobehav. Rev.* **36**, 1640–1645 (2012).

71. C. Sava-Segal, C. Richards, M. Leung, E. S. Finn, Individual differences in neural event segmentation of continuous experiences. *Cereb. Cortex* **33**, 8164–8178 (2023).
72. Y. Ezzyat, L. Davachi, What constitutes an episode in episodic memory? *Psychol. Sci.* **22**, 243–252 (2010).
73. J. Q. Sargent, J. M. Zacks, D. Z. Hambrick, R. T. Zacks, C. A. Kurby, H. R. Bailey, M. L. Eisenberg, T. M. Beck, Event segmentation ability uniquely predicts event memory. *Cognition* **129**, 241–255 (2013).
74. D. H. Brainard, The psychophysics toolbox. *Spat. Vis.* **10**, 433–436 (1997).
75. R. Oostenveld, P. Fries, E. Maris, J.-M. Schoffelen, FieldTrip: Open source software for advanced analysis of MEG, EEG, and invasive electrophysiological data. *Comput. Intell. Neurosci.* **2011**, 156869 (2011).
76. D. M. Groppe, S. Bickel, A. R. Dykstra, X. Wang, P. Mégevand, M. R. Mercier, F. A. Lado, A. D. Mehta, C. J. Honey, iELVis: An open source MATLAB toolbox for localizing and visualizing human intracranial electrode data. *J. Neurosci. Methods* **281**, 40–48 (2017).
77. X. Papademetris, M. P. Jackowski, N. Rajeevan, M. DiStasio, H. Okuda, R. T. Constable, L. H. Staib, BioImage Suite: An integrated medical image analysis suite: An update. *insight J.* **2006**, 209 (2006).
78. B. Fischl, FreeSurfer. *Neuroimage* **62**, 774–781 (2012).
79. M. R. Mercier, S. Bickel, P. Megevand, D. M. Groppe, C. E. Schroeder, A. D. Mehta, F. A. Lado, Evaluation of cortical local field potential diffusion in stereotactic electro-encephalography recordings: A glimpse on white matter signal. *Neuroimage* **147**, 219–232 (2017).
80. J. Q. Kosciessa, T. H. Grandy, D. D. Garrett, M. Werkle-Bergner, Single-trial characterization of neural rhythms: Potential and challenges. *Neuroimage* **206**, 116331 (2020).
81. D. W. Scott, On optimal and data-based histograms. *Biometrika* **66**, 605–610 (1979).

Acknowledgments: We thank the patients for volunteering time and effort to participate in our study. We also thank the Epilepsy Monitoring Staff at the North Shore University Hospital and Lenox Hill Hospital for support. **Funding:** Research reported in this publication was supported by the National Institute of Mental Health of the National Institutes of Health under award numbers F30MH139332 (to A.M.), R01DC019979 (to S.B.), and P50MH109429 (to S.B.). The content is solely the responsibility of the authors and does not necessarily represent the official views of the National Institutes of Health. **Author contributions:** Conceptualization: A.M., G.T., M.N., E.E., C.E.S., A.D.M., and S.B. Methodology: A.M., G.T., M.N., E.E., N.M., A.D.M., and S.B. Investigation: A.M., G.T., M.N., N.M., J.W., E.F., S.G., and M.L. Data curation: A.M., G.T., M.N., E.E., N.M., J.W., E.F., and M.L. Formal analysis: A.M. and G.T. Visualization: A.M., G.T., N.M., and S.B. Writing—original draft: A.M. and S.B. Writing—review and editing: A.M., G.T., M.N., S.G., C.E.S., A.D.M., and S.B. Supervision: A.D.M. and S.B. Project administration: C.E.S., A.D.M., and S.B. Funding acquisition: C.E.S., A.D.M., and S.B. Software: A.M. Resources: C.E.S., A.D.M., and S.B. **Competing interests:** The authors declare that they have no competing interests. **Data and materials availability:** Anonymized data (electrophysiological and behavioral) and all codes required to replicate the main findings of this study can be found at https://doi.org/10.17605/osf.io/dzfpr. All other data needed to evaluate the conclusions in the paper are present in the paper and/or the Supplementary Materials.

Submitted 4 December 2024
Accepted 20 June 2025
Published 25 July 2025
10.1126/sciadv.adv0986